Acta Biomaterialia xxx (2014) xxx–xxx

Contents lists available at ScienceDirect

Acta Biomaterialia

journal homepage: www.elsevier.com/locate/actabiomat

The fabrication of superlow protein absorption zwitterionic coating by electrochemically mediated atom transfer radical polymerization and its application

Yichuan Hu [a,c], Guang Yang [a], Bo Liang [a], Lu Fang [a], Guanglong Ma [b], Qin Zhu [a], Shengfu Chen [b], Xuesong Ye [a,*]

[a] Biosensor National Special Laboratory, Key Laboratory of Biomedical Engineering of Ministry of Education, College of Biomedical Engineering & Instrument Science, Hangzhou 310027, People's Republic of China
[b] State Key Laboratory of Chemical Engineering, Department of Chemical and Biological Engineering, Zhejiang University, Hangzhou 310027, People's Republic of China
[c] Zhijiang College, Zhejiang University of Technology, Hangzhou 310027, People's Republic of China

ARTICLE INFO

Article history:
Received 9 September 2014
Accepted 13 November 2014
Available online xxxx

Keywords:
Electrochemically mediated ATRP
Zwitterionic hydrogel
Nonfouling
Biocompatibility

ABSTRACT

A well-controllable electrochemically mediated surface-initiated atom transfer radical polymerization (e-siATRP) method for the fabrication of superlow protein absorption zwitterionic hydrogel coatings based on poly(sulbetaine methacrylate) (pSBMA) was developed in this work. The effects of the electric condition on polymerization as well as its antifouling performances both in vitro and in vivo were also investigated. Different potentials (−0.08 V, −0.15 V and −0.22 V) and polymerization times (from 8 to 48 h) were chosen to study the polymerization procedure. X-ray photoelectron spectroscopy, atomic force microscopy and ellipsometry measurements were used to characterize the properties of the polymer layers. Ellipsometry measurements showed that a higher potential provided faster polymerization and thicker polymer layers; however, the protein absorption experiments showed that the best polymerization condition was under a constant potential of −0.15 V and 32 h, under which the protein absorption was 0.8% in an enzyme-linked immunosorbent assay (compared to a bare gold electrode). The electrodes with a pSBMA coating effectively deduced the current sensitivity decay both in undiluted serum and in vivo. The usage of the commercially available polymerization monomer of SBMA, the simple convenient synthesis process regardless of the presence of oxygen and the excellent controllability of e-siATRP make it a very promising and universal technique in the preparation of zwitterionic polymer coatings, especially in the development of biocompatible material for implantable devices such as neural and biosensor electrodes.

1. Introduction

The need for implantable medical devices has kept on growing in recent years, with many new devices having been brought to market. Even so, some fundamental obstacles hinder the use of implantable devices in clinical practice, especially with regard to their long-term reliability. Among those obstacles, non-specific protein absorption, also called biofouling, plays a key role [1]. Biofouling begins in the very early stages of implantation. For electronic devices, such as biosensors and neural electrodes, it causes rapid decay in sensitivity. Generally, the procedure of biofouling occurs in the following order: protein adsorption, complement activation, inflammatory cell adhesion. Proteins from plasma, such as albumin, fibrinogen, complement, fibronectin and γ globulin, are involved [2]. Some molecular-level characteristics of surface determined protein adsorption include hydrophilicity, hydrogen-bond acceptors or donors and neutral electrical charge [3]. Therefore, the modification of the surfaces of those electrodes is important. Efforts have been put into anti-biofouling research. Hydrophilic polymers, such as poly(ethylene glycol) (PEG) [4,5] derivatives, polyethylene oxide (PEO) [6], oligo(ethylene glycol) (OEG) [7] and phosphorylcholine (PC) [8], are widely used to reduce non-specific protein absorption. Research from Shen et al. showed that absorption of fibrinogen to plasma deposited PEO was less than 10 ng cm^{-2}, a 20-fold decrease compared to tissue culture polystyrene [9]. But evidence suggested that PEG could decompose in the presence of superoxide anions of H_2O_2, which lead to fouling in the long term [10].

* Corresponding author. Tel.: +86 571 87952756.
E-mail address: yexuesong@zju.edu.cn (X. Ye).

http://dx.doi.org/10.1016/j.actbio.2014.11.023
1742-7061/

In the past few years, zwitterionic hydrogels containing both cationic and anionic groups on the same monomer residue, synthesized by atom transfer radical polymerization (ATRP), showed great properties in repelling protein [11–13], anti-cell adhesion [14,15] and biosensing [16,17]. In Yang et al.'s research, surfaces with 62 nm poly(sulbetaine methacrylate) (pSBMA) brushes presented the best nonfouling character with protein adsorption of 6 ng cm^{-2} [18]. Chang et al. enhanced this to less than 2 ng cm^{-2} in diluted plasma solution [19], while in the experiment of Li et al., pSBMA coated surface had very low nonspecific protein adsorption levels of 0.8 ng cm^{-2} from 100% human serum [20]. Furthermore, the well-defined copolymerization of poly(SBMA) with poly(propylene oxide) (PPO) reduced protein adsorption to 3 ng cm^{-2} [21]. Poly (carboxybetaine methacrylate) (polyCBMA) reduced single protein absorption to 0.3 ng cm^{-2} [22]. The data from Vaisocherová et al. showed that a thin layer of poly(carboxybetaine acrylamide) (pCBAA) on gold-coated substrates achieved almost no non-specific protein absorption in undiluted human blood serum [23]. Recently, functionable polycarboxybetaine acrylamide (pCB), which created high polymer packing densities on the surface, was found to have a super low adsorption of <0.3 ng cm^{-2} [24]. Moreover, zwitterionic gel showed excellent bacteria-repellent properties as well [25–27].

ATRP is conducted by an active equilibrium between lower and higher oxidation states of a transit metal complex. These complexes combine metal ions and corresponding ligands, which provide radicals, then promote monomer addition. The speed of polymerization of monomers is effectively controlled by the concentration of radicals, which is regulated by the ratio of the lower state to the higher state of metal activators. Then the higher state oxidation deactivator terminates propagation. ATRP provides highly uniform nano-brush-like surfaces, giving those polymers particular features. Most of those experiments based on ATRP require careful handling: an O_2-free environment, anhydrous operation, and so on. All of those inconveniences restrain the wide application of zwitterionic hydrogels, especially in the development of biomedical devices, such as enzyme electrodes.

In recent years, a new kind of ATRP, electrochemically mediated ATRP (eATRP), was introduced [28] and comprehensively inspected. Applied potential becomes a key force that promotes polymerization [29]. Soon after, electrochemically induced surface-initiated ATRP (e-siATRP) was developed [30]. Scheme 1 shows the mechanism of polymer brush growth using e-siATRP. The reaction was carried out in an electrochemical cell with a two- or three-electrode system. A constant potential was applied to generate the Cu^{I} complex through one-electron reduction of Cu^{II}/bipyridine (bpy) in the vicinity of the initiator-decorated gold surface to initiate the polymerization. e-siATRP is a powerful method which could control the whole procedure of polymerization by precisely manipulating the ratio of Cu^{I}/Cu^{II} through tuning applied potentials and the distance of catalysis complex diffusion [31]. As a universal and convenient ATRP method, e-siATRP of zwitterionic gel shows a broad prospect in functional biomaterials preparation.

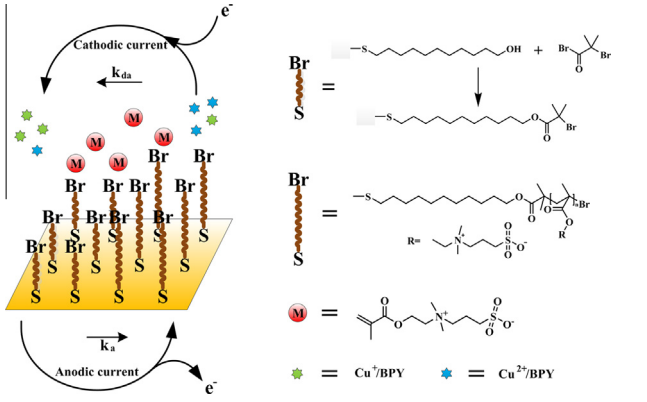

Scheme 1. Mechanism of electrochemically induced si-ATRP at a cathodic current to generate the $Cu^{I}Cl$/BPY complex that triggers the polymerization. (K_a and K_{da} represent the rate constants of activation and deactivation propagation, respectively).

In the previous research, most of the zwitterionic gels showing great antifouling performance were synthesized by conventional ATRP. However, those monomers such as CBMA, CBAA, and CB are not commercially available. In this work, in order to demonstrate a universal approach to prepare antifouling coating, a commercially available zwitterionic monomer, SBMA, was chosen as the model monomer. For the first time, e-siATRP was applied to polymerize zwitterionic gel on gold electrodes potentially used as implantable devices. The effects of electric condition to polymerization were investigated and the thicknesses of pSBMA coating on Au-covered silicon wafers were measured by ellipsometry to discover the relationship between anti-biofouling performance and the thickness of the polymer layers under different electrical conditions. The antifouling performances both in vitro and in vivo were also investigated. Compared with traditional material, such as PU, pSBMA coating showed better performance.

2. Experimental methods

2.1. Materials and instruments

N-(3-sulfopropyl)-N-(methacryloxyethyl)-N, N-dimethyl ammonium betaine (SBMA, 97%), bromoisobu-tyryl bromide (BIBB, 98%), 11-mercapto-1-undecanol (97%), 2,2′-bipyridine (bpy, 99%) were purchased from Sigma-Aldrich (Milwaukee, USA). Benzyltri-n-butylammonium chloride (BBAC, 98%) was purchased from Alfa Aesar (Tianjin, China). Copper chloride (AP), methanol (AP) and tetrahydrofuran (THF, HPLC grade) were purchased from Aladdin (Shanghai, China). Biotin-labeled goat anti-mouse IgG (H + L), HRP-labeled streptavidin and TMB horseradish peroxidase color development solution were purchased from Beyotime (Shanghai, China). Gold wire (99.999%) was purchased from New-Metal (Beijing, China). Other regular chemicals used were of analytical reagent grade, purchased from Sinopharm (Shanghai, China).

Electropolymerization and electrochemical measurements were performed with an electrochemical workstation (μAutolab III, Metrohm, Switzerland). Scanning electron microscopy images were collected on a thermal field emission scanning electron microscope (FEI SIRION-100, The Netherlands). All electrochemical experiments were carried out at room temperature.

2.2. Synthesis of initiator

ω-Mercaptoundecyl bromoisobutyrate (Br-thiol) was synthesized through reaction of BIBB and 11-mercapto-1-undecanol using a method published previously [11,32]. The product after purification was a colorless viscous liquid (0.79 g ml^{-1}). Nuclear magnetic resonance (NMR) was recorded using deuterated methanol as the solvent. (Proton nuclear magnetic resonance (^{1}H NMR) (400 MHz, $CDCl_3$): 4.15 (*t*, *J* = 6.9, 2H, OCH_2), 2.51 (*q*, *J* = 7.5, 2H, SCH_2), 1.92 (s, 6H, CH_3), 1.57–1.72 (m, 4H, CH_2) and 1.24–1.40 (m, 16H, CH_2)).

2.3. Preparation of Au–Si working electrodes

Double-sided polished Si wafers were cut into sticks of 1 × 20 × 0.4 mm (width × length × thickness). After thorough rinsing with acetone and anhydrous ethyl alcohol, the sticks were put in a customized Teflon fixture closely side by side, exposing

Please cite this article in press as: Hu Y et al. The fabrication of superlow protein absorption zwitterionic coating by electrochemically mediated atom transfer radical polymerization and its application. Acta Biomater (2014), http://dx.doi.org/10.1016/j.actbio.2014.11.023

one face only. Then 5–7 nm thick titanium and 100 nm thick gold were evaporated by an electron beam evaporation deposition system (ABGCZD11036 Angstrom Engineering Inc., USA). After evaporation on one face, the sticks were turned in order to expose another face, then the evaporation procedure was repeated again until five faces of the sticks were coated by gold film.

2.4. SAM of initiator

First, Au–Si electrodes and standard Au disk electrodes were carefully rinsed in acetone, anhydrous ethyl alcohol and deionized water in sequence, then dried with a nitrogen stream. Secondly, all those electrodes were soaked in chromic acid (10% potassium dichromate in 25% sulfuric acid) for at least 4 h, followed by a careful rinse with deionized water, and again dried with a nitrogen stream. The immobilization of thiol ester initiators was prepared by immersing Au–Si electrodes into 2 mM initiator solution in ethanol for at least 18 h at room temperature. Before e-siATRP, each electrode was thoroughly rinsed with THF, ethanol and deionized water in sequence. Carefully cleaned Au disk electrodes were dipped into 3% PU/THF for 3 s and dried in air, serving as control in the following experiments.

2.5. Conduction of e-siATRP

Electrochemically induced surface-initiated ATRP is carried with a traditional three-electrode system in 15 ml of 0.1 M BBAC buffer, with 3 M SBMA, 60 mM bpy and 30 mM $CuCl_2$ (the mole ratio of monomer:ligand:Cu = 100:2:1). Cyclic voltammetry (CVA) was applied under the potential range of −0.8 V and 0.4 V at 100 mV s^{-1} (vs. Ag/AgCl). Then three different applied potentials were chosen to inspect their effects in constant potential polymerization.

2.6. Protein absorption and enzyme-linked immunosorbent assay (ELISA)

Prepared pSBMA-Au–Si electrodes were immersed in a 0.1 mg ml^{-1} biotin-labeled goat anti-mouse IgG solution for 2 h, at 37 °C. Then, the substrates were rinsed five times with 0.01 M phosphate-buffered saline (PBS) and incubated in bovine serum albumin (BSA; 1 mg ml^{-1} in PBS) solution for 90 min at 37 °C to block the areas unoccupied by antibodies. After being rinsed five times by the PBS solution, all electrodes were treated by HRP-streptavidin for 30 min, at a 1/2000 dilution, and rinsed again. After that, electrodes were transferred to clean microcentrifuge tubes and incubated with 200 μl of 0.01 M PBS containing TMB horseradish peroxidase for 20 min at 37 °C. The enzyme-induced color reaction was stopped by adding 50 μl of 2 M H_2SO_4 to the solution in each tube. Finally, the absorbance of light intensity at 450 nm was determined by a microplate reader. The absorbance from a bare Au–Si electrode is equivalent to 100% for calculating relative adsorption values.

2.7. Ellipsometry analysis

After electropolymerization, ellipsometry was performed with a spectroscopic ellipsometer (J. A. Woollam, M-2000). Five separate spots were measured at three different angles of incidence (50°, 60° and 70°). Bare Au–Si wafers were used as reference. The thicknesses of films were determined using the Cauchy layer model with an assumed refractive index of 1.42.

2.8. Electrochemical impedance spectroscopy (EIS) assay and impedance–time scan

EIS was carried out using an electrochemical workstation (μAutolab III, Metrohm, Switzerland) at an open circuit potential and 1 mV AC potential was applied; the voltage frequencies ranged from 0.1 Hz to 10^5 Hz in the presence of a 1 mM $K_3(Fe(CN)_6)/K_4(Fe(CN)_6)$ (1:1) mixture as a redox probe in 0.1 M K_2SO_4 solution. A conventional three-electrode cell was used: platinum disk counter electrode, prepared pSBMA-Au disk working electrode and Ag/AgCl reference electrode. An in vitro impedance–time scan was carried in undiluted bovine serum at 37 °C.

In vivo animal experiments were carried out according to the national guidelines for the care and use of laboratory animals in China. Five male Sprague–Dawley rats weighting ~200 g were anesthetized by intraperitoneal injection of pentobarbital sodium solution (30 mg kg^{-1}). Symmetrical incisions ~1 cm long were made on dorsal regions of the rats lateral to the spine, followed by the creation of subcutaneous pouches by blunt dissection with forceps. A small piece of printed circuit board with three parallel arranged electrodes (platinum wire counter electrode, prepared pSBMA Au–Si working electrode, and Ag/AgCl wire reference electrode) was inserted in the pouches. Electrodes were subject to a 1 kHz interrogating sine wave of 50 mV peak-to-peak voltage [33]. The impedance of each electrode was monitored over time.

3. Results and discussion

3.1. Preparation of self-assembled monolayer (SAM) decorated Au–Si electrodes

The preparation of SAMs is a convenient method to prepare surfaces for siATRP, especially on gold. The choice of initiator has a strong effect on polymerization. In the research of Li et al. [30], the long chain initiator SH-C15-Br decorated gold electrode showed a very large impedance (71 kΩ cm^{-2}) of the monolayer to charge transfer. The SAM of short chain alkanethiols is known to be of low resistance but poorly packed, which leads to a defect-rich and a limited polymer layer. In order to achieve homogeneous films, SH-C15-Br was mixed with 2-thionaphthil (2-NAT) in the ratio of 10:1 as the ultimate initiator. That strategy reduced the surface impedance to 2.47 kΩ cm^{-2}, and provided a high-quality SAM layer for e-ATRP. In this paper, a stick type Si with Au coating was chosen to be the electrode and a C11 initiator, ω-mercaptoundecyl bromoisobutyrate, was synthesized following previous reports [32]. Prior to polymerization, EIS was carried to inspect the charge transfer resistance

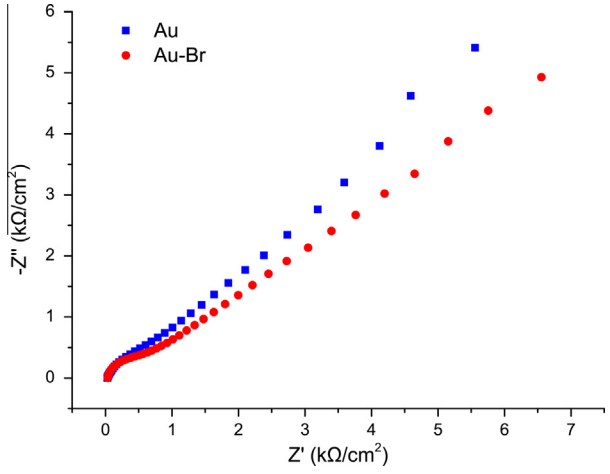

Fig. 1. EIS plots of bare gold and initiator treated gold (Au–Br) electrode.

Please cite this article in press as: Hu Y et al. The fabrication of superlow protein absorption zwitterionic coating by electrochemically mediated atom transfer radical polymerization and its application. Acta Biomater (2014), http://dx.doi.org/10.1016/j.actbio.2014.11.023

(R_{ct}) of gold electrodes. Compared to the results of Li et al., the interfacial R_{ct} (less than 1 kΩ cm^{-2}) of C11 initiator layers was much lower, as shown in Fig. 1. Therefore, no short chain alkanethiols were needed in the initiator solution. Little difference was seen in subsequent experiments.

3.2. Electrochemistry performance

Fig. 2 shows the cyclic voltammetry curve of the SBMA/BPY/$CuCl_2$ complex in H_2O/MeOH. A pair of reversible peaks appeared at E_{pc} = 0.22 V; E_{pa} = 0.01 V vs. the standard Ag/AgCl electrode only

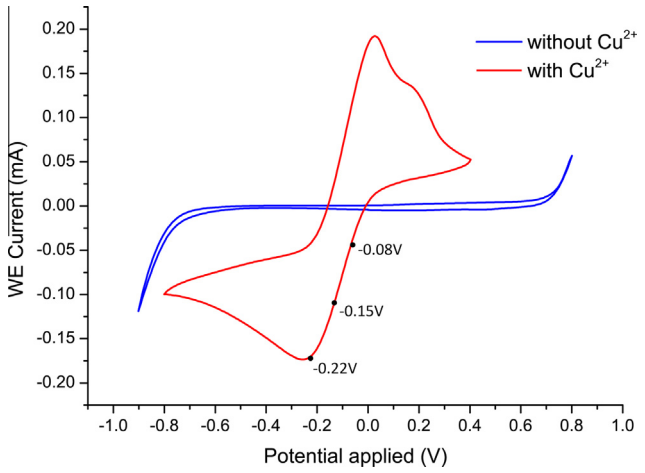

Fig. 2. CVA of 15 ml solution of H_2O/MeOH (2:1, v/v) at 25 °C, containing [SBMA] = 3 M, [BBAC] = 0.1 M, [SBMA]:[BPY]:[$CuCl_2$] = 100:2:1, scan rate: v = 0.1 V s^{-1}. The three points correspond to the E_{app} used in the polymerization.

when Cu^{II} was added. Unlike "conventional" ATRP, which is triggered by adding $Cu^{I}X$ (X = Br, Cl) and determined by the ratio of [Cu^{I}]/[Cu^{II}], e-ATRP is an electrochemistry process driven by $\Delta G^{o} = F(E_{app} - E^{0'})$. Before the potential is applied, the reaction system contains monomer, ligand and initiator, but no Cu^{I} exits, so no polymerization occurs. When a sufficient potential is applied, Cu^{II} reduces to Cu^{I}, and Cu^{I}/Ligand activates the polymerization [28]. During the propagation of the polymer, Cu^{I}/Ligand contributes an electron to the monomer and turns it to [R·], then converts to Cu^{II}/Ligand, preparing for the next cycle. The ratio of [Cu^{I}/Ligand]/[Cu^{II}/Ligand] determines the proceeding of ATRP directly. In "conventional" ATRP, this ratio is controlled by [Cu^{I}] added in the polymerization system. But Cu^{I} is so unstable that it is oxidized very quickly in the presence of oxygen. That is why oxygen-free operation is so crucial in traditional ATRP, whereas in e-ATRP, we can easily adjust it by tuning the applied potential. Here, a higher ΔG^{o} provides a larger ratio of [Cu^{I}/Ligand]/[Cu^{II}/Ligand], and therefore pushes a faster propagation on the surface of the working electrode. As a living polymerization, the process of e-ATRP could be ensured by a precisely tuned applied potential. In our experiments, three different applied potentials were chosen to inspect their effects on polymerization.

As shown in Fig. 2, the maximum reduction current appeared at −0.22 V. At this point, the ratio of [Cu^{I}/Ligand]/[Cu^{II}/Ligand] ⩾ 1 [28]; Cu^{I}/Ligand regenerated faster than Cu^{II}/Ligand. Therefore, polymers grew faster than at the middle applied potential, −0.15 V. We also picked a more positive potential, −0.08 V, which is very close to the "switch-off point" to demonstrate the relationship of applied potential with polymerization. At this point, the growth of polymers was even slower. The final thickness of polymers showed the same result, as shown in Fig. 6A. Basically, polymers grew monotonously at the first level in the first several hours

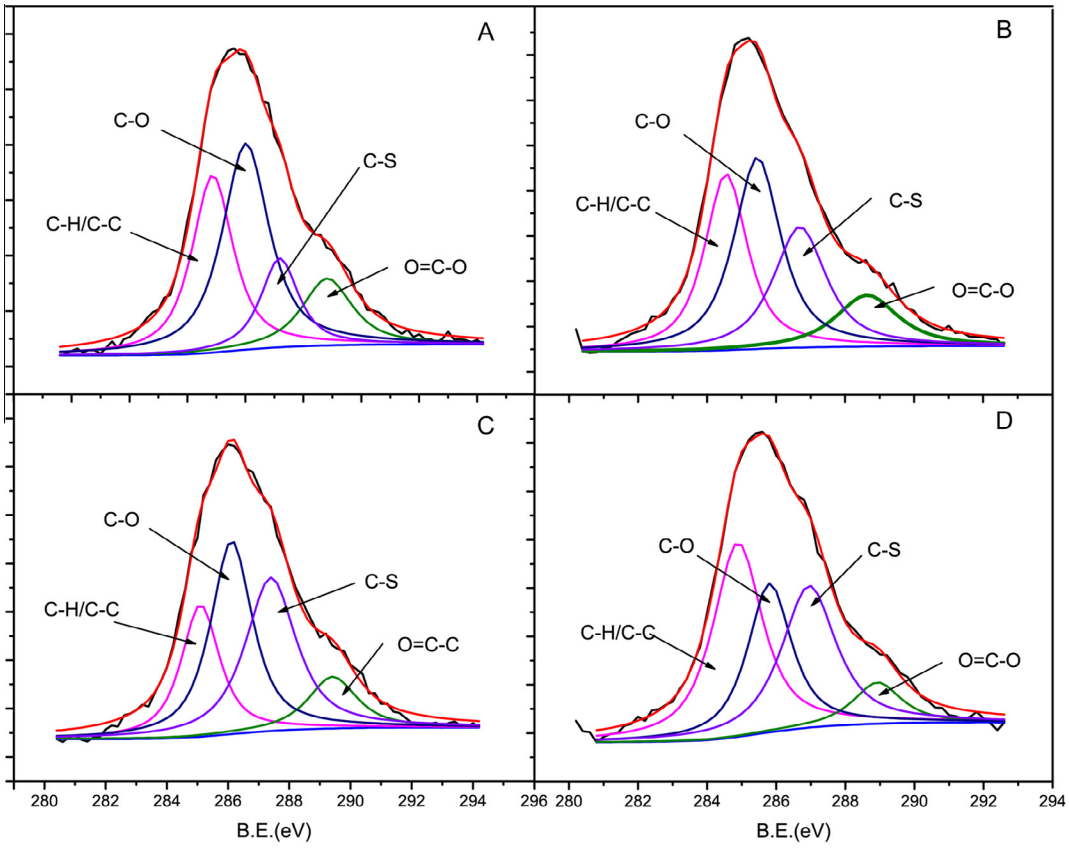

Fig. 3. High-resolution scan of C_{1s} spectrum of pSBMA-Au electrodes with different polymerization time. (A) Au electrode after being treated with initiator; (B–D) pSBMA-Au electrodes with 4, 8, 12 h polymerization, respectively.

Please cite this article in press as: Hu Y et al. The fabrication of superlow protein absorption zwitterionic coating by electrochemically mediated atom transfer radical polymerization and its application. Acta Biomater (2014), http://dx.doi.org/10.1016/j.actbio.2014.11.023

and then leveled off after 24 h. At all three applied potential conditions, the final polymer thicknesses showed a similar linear relationship with polymerization time. This result is in accord with the research of Magenau et al. [34].

3.3. Polymerization of pSBMA

On the basis of Scheme 1, the pSBMA Au–Si electrode is constructed via a surface immobilized initiator and e-siATRP of SBMA. The presence of grafted sulbetaine moieties was ascertained by X-ray photoelectron spectroscopy analysis. As shown in Fig. 3, in the curve-fitted C_{1s} spectrum, C–S peak component, at the Binding Energy (BE) of 287 eV, is associated with both the sulfa group of the SBMA monomer and the sulfhydryl between Au and initiator [35]. The proportion of C–S in C_{1s} kept growing during polymerization, from 4 h to 12 h, indicating that SBMA was polymerized on the surfaces of Au electrodes. Because of the poor conductivity of pSBMA, the interfacial resistance of the electrode with thicker polymers is larger than that of thinner ones. The EIS plot confirmed this (Fig. 4).

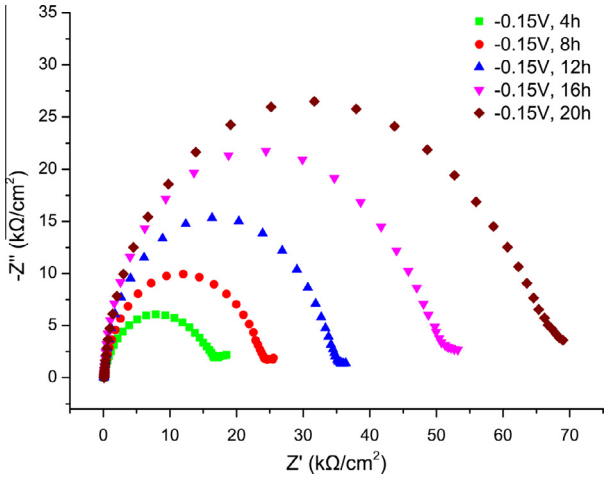

Fig. 4. Impedance plots of different polymer layers in 0.1 M K_2SO_4 and 1 mM $K_3[Fe(CN)_6]/K_4[Fe(CN)_6]$.

Atomic force microscopy (AFM) images reveal morphological features of pSBMA Au–Si electrodes. In Fig. 5A, evaporated gold formed a homogeneous layer with flat bumps, varying in size from 200 to 400 nm, on the surface of bare Au–Si electrode. The roughness of the gold layer was ~5–10 nm. In Fig. 5B, the surface of electrodes coated with pSBMA results in a cover layer of smaller bumps, closely packed, mostly within 100 nm. The roughness of the pSBMA brush was ~10–30 nm.

The growth of polymers is affected by applied potential. Higher potential brings faster growth of the polymer brush, as shown in Fig. 6A. In our experiments, in the first few hours (<10 h), all polymerization processions appeared as a first-order plot, but leveled off after 20 h. A higher potential makes polymer layers grow faster and thicker. As it revealed, certain thickness of the polymer layer can be achieved by applying the corresponding potential with this well-controllable technique, as for other zwitterionic monomers.

3.4. Antifouling performance

In this work, the anti-biofouling performance of pSBMA coating was analyzed by ELISA at 37 °C. Fig. 6B–D presents the relationship

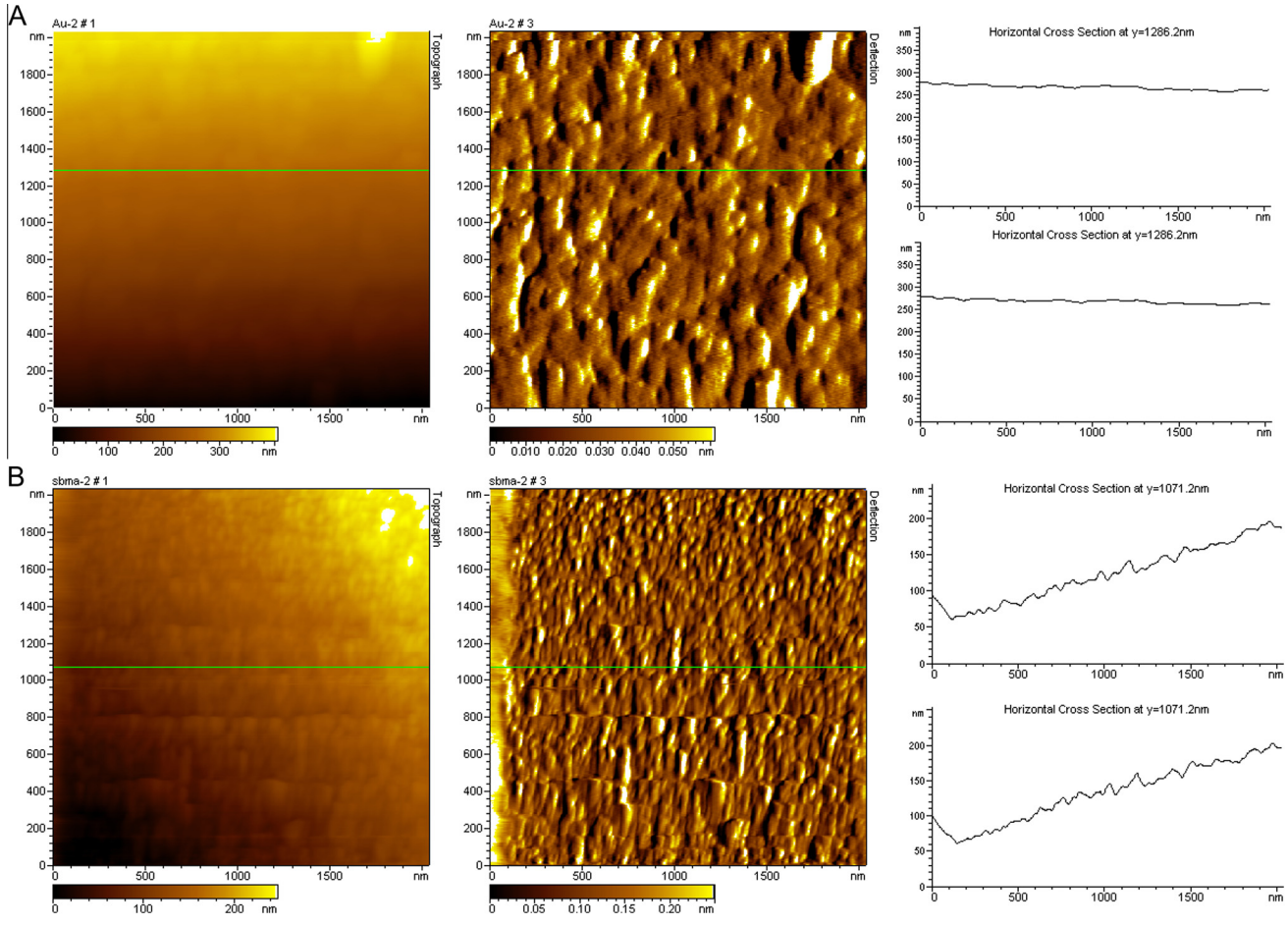

Fig. 5. AFM image of Au–Si electrode without (A) and with pSBMA (B) of 32 h polymerization under −0.15 V.

Please cite this article in press as: Hu Y et al. The fabrication of superlow protein absorption zwitterionic coating by electrochemically mediated atom transfer radical polymerization and its application. Acta Biomater (2014), http://dx.doi.org/10.1016/j.actbio.2014.11.023

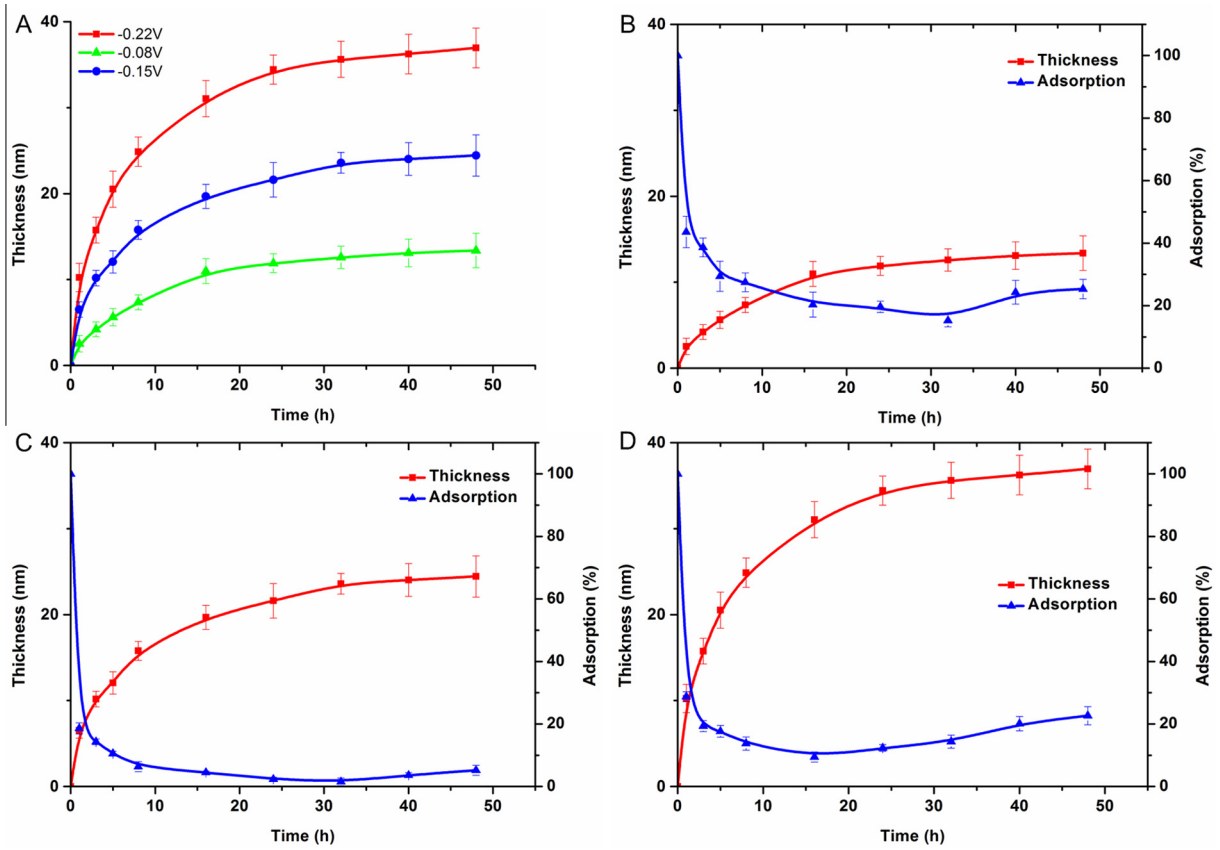

Fig. 6. Polymer thickness under different electroconditions (A) and the relationship between anti-biofouling performance and the thickness of the polymer layers with electroconditions (which are −0.08 V, −0.15 V and −0.22 V respectively) (B–D).

between antifouling performance and the thickness of the polymer layers with electroconditions. pSBMA coating showed good resistance to protein absorption in all cases. Under the applied potential of −0.15 V, the relative absorption of protein on the pSBMA-Au–Si surface reduced to 0.8% of the positive control bare Au–Si surface after 32 h polymerization and the calculated protein absorption was ~2.2 ng cm^{-2}, which is better than the result of Yang et al. (a full monolayer of absorbed protein on the surface is equivalent to 270 ng cm^{-2} [20]) [18]. The lowest absorption was less than 0.6%, in unshown data. The corresponding thickness of pSBMA is 23 nm. While under the potential of −0.22 V, the pSBMA coating reached its lowest protein-absorption point, ~11.2% of the control, with a thickness of 31 nm. In our experiments, antifouling performance is not thickness-dependent. For instance, at the thickness of 12 nm, ~30% protein was absorbed under −0.22 V, but 18% and 10% resistance for −0.08 V and −0.15 V, respectively. When the thickness grew to 23 nm, the pSBMA coating showed the best antifouling performance, resisting 99% protein adsorption under −0.15 V applied potential. In all three applied potentials, protein adsorption declined with growing thickness, but increased when growth exceeded a certain point. It suggested that the best antifouling performance came from a good balance between grow rate and polymer layer thickness.

As has been previously proved, one of the most important characteristics of antifouling surface is hydrophilicity [36], which is determined by the interaction of adjacent polymer chains. High packing density contributes to form a uniform polymer brush, consequently helping to achieve better hydrophilicity [37]. Faster growth, however, brings lower packing density, which leads to worse antifouling performance. Thickness is another key factor. In the first hour of polymerization, protein adsorption was rather high with thin polymer layers. But if the layer of polymers gets too thick, defects and wrinkles may appear and lead to a protein absorption increase again [38,39]. In our cases, higher applied potential induced faster polymer growth and subsequently increased protein adsorption.

SBMA is a commercialized zwitterionic monomer which has been extensively studied in recent years. In Yang's research, surfaces with 62 nm pSBMA brushes presented the best nonfouling character of 6 ng cm^{-2} [18]. It has been reported that an initiator with a catechol end group for surface anchoring was robust, and a NH_2-treated pSBMA gold surface achieved ultralow fouling (<5 ng cm^{-2}) [20]. In the work of Tah and Bernard, a copolymer, [2-(acryloyloxy) ethyl] trimethyl ammonium chloride (TMA):[2-(acryloyloxy) ethyl] trimethyl ammonium chloride (CAA), obtained a 0.5% absorption with the thickness of ~18 nm, after over 24 h reaction [40]. When mixed with acrylic acid (AA) at a ratio of 56:44, pSBMA-pAA coating reached the lowest absorption of 3% [41]. Under optimized conditions, PSA-b-PSBMA coated surfaces can strongly resist non-specific protein adsorption both in single protein solution and in human whole blood [42]. Some carboxybetaine zwitterionic gel demonstrated better anti-biofouling features, even in a complex medium [43] such as pCBAA, which achieved a super-low protein absorption of less than 0.3 ng cm^{-2} with a thickness of 21 nm in single protein solution, in Yang et al.'s work [13,18]. Because of the key role of polymer density, Gao et al. group recently synthesized a new polymer, poly(carboxybetaine) (pCB), with two catechol groups for anchoring and two chains for creating high polymer packing densities on the surface, then achieving a super low absorption of <0.3 ng cm^{-2}, with a thickness of 10 nm [24]. Furthermore, Huang et al. controlled hierarchical architecture of pCB, successfully combining ultralow fouling with high loading properties via siATRP [44].

Please cite this article in press as: Hu Y et al. The fabrication of superlow protein absorption zwitterionic coating by electrochemically mediated atom transfer radical polymerization and its application. Acta Biomater (2014), http://dx.doi.org/10.1016/j.actbio.2014.11.023

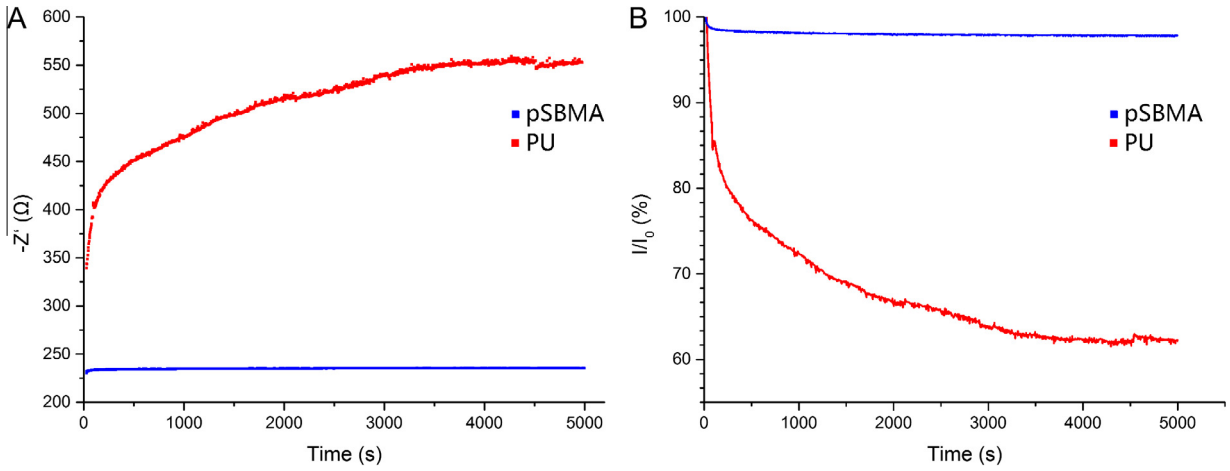

Fig. 7. The effect of pSBMA coating (32 h polymerization under −0.15 V) to electrode performance in undiluted serum in 37 °C. (A) Impedance–time scan; (B) sensitivity decay curve.

3.5. The effect of pSBMA coating to electrode performance in vitro and in vivo

In the application of biosensors and neural electrodes, passivation induced by biofouling decreases the responses of electrodevices [2]. One way to inspect electrode performance is impedance–time scans [45]. In vitro scans were proceeded in undiluted bovine serum at 37 °C. The curves showed that impedances of both electrodes with PU coating and with pSBMA coating increased in the first few minutes. The latter equilibrated very quickly after that, while it took almost 1 h for the former to achieve a balance, see Fig. 7A. The rate of input current to output current (I/I_0) represents the stability of an electrodevice. As shown in Fig. 7B, the response of the PU coated electrode decayed 37% in 1 h, while the response of the electrode with pSBMA decayed only ~2%, demonstrating excellent antifouling performance in complex medium. Further in vivo tests verified similar appearances; results are shown in Fig. 8. In the application of implantable devices, such as implantable neural or biosensor electrodes, in vivo biological signal detections are susceptible to the stability of the electrical characteristics [46,47]. The coating of pSBMA effectively reduced the change of the electrode impedance induced by protein absorption, showing promising applications in implantable devices. In further research, e-siATRP of SBMA could be incorporated into the development of implantable biosensors to improve the overall performance in vivo.

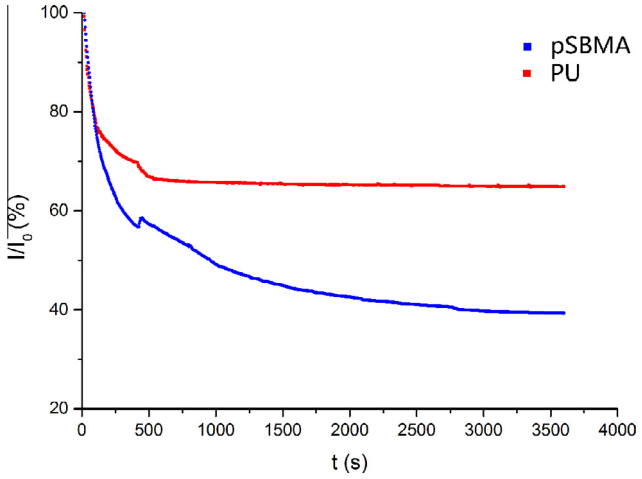

Fig. 8. The effect of pSBMA coating (32 h polymerization under −0.15 V) to electrode performance in vivo.

4. Conclusion

In this work, for the first time, e-siATRP was applied to polymerize a zwitterionic monomer, SBMA, on gold electrodes and great anti-biofouling performances were achieved. The relationship between anti-biofouling performance and electroconditions was inspected as well. Our results revealed that the polymerization procedure could be easily controlled by tuning electroconditions and the thicknesses of polymers were determined by the applied potential. Protein absorption was reduced to 0.8% in ELISA, which is a better result than most of the previous research. Electro-induced polymerization may provide homogeneous circumstances and precise control of Cu^+, which leads to excellent polymerization. Further, in vitro and in vivo impedance–time scans showed that pSBMA coating effectively delayed the sensitivity decay of electrodes. Because of the good availability of SBMA and the easy handling of e-siATRP, this method has great potential in the preparation of zwitterionic polymer coatings, especially in the development of implantable devices.

Acknowledgments

This work was financially supported by the National Key Technology R&D Program of China and the National Natural Science Foundation of China (Nos. 81171416, 60875078).

Appendix A. Figures with essential colour discrimination

Certain figure in this article, particularly Figs. 1–8 is difficult to interpret in black and white. The full colour images can be found in the on-line version, at http://dx.doi.org/10.1016/j.actbio.2014.11.023.

References

[1] Rabe M, Verdes D, Seeger S. Understanding protein adsorption phenomena at solid surfaces. Adv Colloid Interface Sci 2011;162:87–106.
[2] Anderson JM, Rodriguez A, Chang DT. Foreign body reaction to biomaterials. Semin Immunol 2008;20:86–100.
[3] Chapman RG, Ostuni E, Takayama S, Holmlin RE, Yan L, Whitesides GM. Surveying for surfaces that resist the adsorption of proteins. J Am Chem Soc 2000;122:8303–4.

[4] Li L, Chen S, Zheng J, Ratner BD, Jiang S. Protein adsorption on oligo(ethylene glycol)-terminated alkanethiol self-assembled monolayers: the molecular basis for nonfouling behavior. J Phys Chem B 2005;109:2934–41.
[5] Dalsin JL, Hu B-H, Lee BP, Messersmith PB. Mussel adhesive protein mimetic polymers for the preparation of nonfouling surfaces. J Am Chem Soc 2003;125:4253–8.
[6] Prime KL, Whitesides GM. Self-assembled organic monolayers: model systems for studying adsorption of proteins at surfaces. Science 1991;252:1164–7.
[7] Zheng J, Li L, Chen S, Jiang S. Molecular simulation study of water interactions with oligo (ethylene glycol)-terminated alkanethiol self-assembled monolayers. Langmuir 2004;20:8931–8.
[8] Chen S, Zheng J, Li L, Jiang S. Strong resistance of phosphorylcholine self-assembled monolayers to protein adsorption: insights into nonfouling properties of zwitterionic materials. J Am Chem Soc 2005;127:14473–8.
[9] Shen M, Martinson L, Wagner MS, Castner DG, Ratner BD, Horbett TA. PEO-like plasma polymerized tetraglyme surface interactions with leukocytes and proteins: in vitro and in vivo studies. J Biomater Sci, Polym Ed 2002;13:367–90.
[10] Hu T, Li D, Manjula BN, Acharya SA. Autoxidation of the site-specifically PEGylated hemoglobins: role of the PEG chains and the sites of PEGylation in the autoxidation. Biochemistry 2008;47:10981–90.
[11] Zhang Z, Chen S, Chang Y, Jiang S. Surface grafted sulfobetaine polymers via atom transfer radical polymerization as superlow fouling coatings. J Phys Chem B 2006;110:10799–804.
[12] Chen S, Jiang S. A new avenue to nonfouling materials. Adv Mater 2008;20:335–8.
[13] Yang W, Xue H, Li W, Zhang JL, Jiang SY. Pursuing "zero" protein adsorption of poly(carboxybetaine) from undiluted blood serum and plasma. Langmuir 2009;25:11911–6.
[14] Cheng G, Li GZ, Xue H, Chen SF, Bryers JD, Jiang SY. Zwitterionic carboxybetaine polymer surfaces and their resistance to long-term biofilm formation. Biomaterials 2009;30:5234–40.
[15] Jiang S, Cao Z. Ultralow-Fouling, functionalizable, and hydrolyzable zwitterionic materials and their derivatives for biological applications. Adv Mater 2010;22:920–32.
[16] Wu YF, Liu SQ, He L. Electrochemical biosensing using amplification-by-polymerization. Anal Chem 2009;81:7015–21.
[17] Yang W, Bai T, Carr LR, Keefe AJ, Xu J, Xue H, et al. The effect of lightly crosslinked poly(carboxybetaine) hydrogel coating on the performance of sensors in whole blood. Biomaterials 2012;33:7945–51.
[18] Yang W, Chen S, Cheng G, Vaisocherová H, Xue H, Li W, et al. Film thickness dependence of protein adsorption from blood serum and plasma onto poly(sulfobetaine)-grafted surfaces. Langmuir 2008;24:9211–4.
[19] Chang Y, Liao S-C, Higuchi A, Ruaan R-C, Chu C-W, Chen W-Y. A highly stable nonbiofouling surface with well-packed grafted zwitterionic polysulfobetaine for plasma protein repulsion. Langmuir 2008;24:5453–8.
[20] Li G, Xue H, Cheng G, Chen S, Zhang F, Jiang S. Ultralow fouling zwitterionic polymers grafted from surfaces covered with an initiator via an adhesive mussel mimetic linkage. J Phys Chem B 2008;112:15269–74.
[21] Chang Y, Chen S, Zhang Z, Jiang S. Highly protein-resistant coatings from well-defined diblock copolymers containing sulfobetaines. Langmuir 2006;22:2222–6.
[22] Zhang Z, Chen S, Jiang S. Dual-functional biomimetic materials: nonfouling poly(carboxybetaine) with active functional groups for protein immobilization. Biomacromolecules 2006;7:3311–5.
[23] Vaisocherová H, Yang W, Zhang Z, Cao Z, Cheng G, Piliarik M, et al. Ultralow fouling and functionalizable surface chemistry based on a zwitterionic polymer enabling sensitive and specific protein detection in undiluted blood plasma. Anal Chem 2008;80:7894–901.
[24] Gao CL, Li GZ, Xue H, Yang W, Zhang FB, Jiang SY. Functionalizable and ultra-low fouling zwitterionic surfaces via adhesive mussel mimetic linkages. Biomaterials 2010;31:1486–92.
[25] Laloyaux X, Fautré E, Blin T, Purohit V, Leprince J, Jouenne T, et al. Temperature-responsive polymer brushes switching from bactericidal to cell-repellent. Adv Mater 2010;22:5024–8.
[26] Cao Z, Mi L, Mendiola J, Ella-Menye J-R, Zhang L, Xue H, et al. Reversibly switching the function of a surface between attacking and defending against bacteria. Angew Chem 2012;124:2656–9.
[27] Cheng G, Xue H, Zhang Z, Chen S, Jiang S. A switchable biocompatible polymer surface with self-sterilizing and nonfouling capabilities. Angew Chem 2008;120:8963–6.
[28] Magenau AJD, Strandwitz NC, Gennaro A, Matyjaszewski K. Electrochemically mediated atom transfer radical polymerization. Science 2011;332:81–4.
[29] Bortolamei N, Isse AA, Magenau AJD, Gennaro A, Matyjaszewski K. Controlled aqueous atom transfer radical polymerization with electrochemical generation of the active catalyst. Angew Chem, Int Ed 2011;50:11391–4.
[30] Li B, Yu B, Huck WTS, Zhou F, Liu W. Electrochemically induced surface-initiated atom-transfer radical polymerization. Angew Chem 2012;124:5182–5.
[31] Yan J, Li B, Yu B, Huck WTS, Liu W, Zhou F. Controlled polymer-brush growth from microliter volumes using sacrificial-anode atom-transfer radical polymerization. Angew Chem, Int Ed 2013;52:9125–9.
[32] Jones DM, Brown AA, Huck WTS. Surface-initiated polymerizations in aqueous media: effect of initiator density. Langmuir 2002;18:1265–9.
[33] Suner S, Fellows MR, Vargas-Irwin C, Nakata GK, Donoghue JP. Reliability of signals from a chronically implanted, silicon-based electrode array in non-human primate primary motor cortex. IEEE Trans Neural Syst Rehabil Eng 2005;13:524–41.
[34] Magenau AJD, Bortolamei N, Frick E, Park S, Gennaro A, Matyjaszewski K. Investigation of electrochemically mediated atom transfer radical polymerization. Macromolecules 2013;46:4346–53.
[35] Wagner DC, Riggs WM, Davis LE, Moulder JF. Handbook of X-ray photoelectron spectroscopy. Eden Prairie, MN: Perkin-Elmer Corporation; 1979.
[36] Ostuni E, Chapman RG, Holmlin RE, Takayama S, Whitesides GM. A survey of structure–property relationships of surfaces that resist the adsorption of protein. Langmuir 2001;17:5605–20.
[37] Huang C-J, Li Y, Krause JB, Brault ND, Jiang S. Internal architecture of zwitterionic polymer brushes regulates nonfouling properties. Macromol Rapid Commun 2012;33:1003–7.
[38] Zhao C, Li L, Wang Q, Yu Q, Zheng J. Effect of film thickness on the antifouling performance of poly(hydroxy-functional methacrylates) grafted surfaces. Langmuir 2011;27:4906–13.
[39] Cheng N, Brown AA, Azzaroni O, Huck WTS. Thickness-dependent properties of polyzwitterionic brushes. Macromolecules 2008;41:6317–21.
[40] Tah T, Bernards MT. Nonfouling polyampholyte polymer brushes with protein conjugation capacity. Colloids Surf, B 2012;93:195–201.
[41] Kuo W-H, Wang M-J, Chien H-W, Wei T-C, Lee C, Tsai W-B. Surface modification with poly(sulfobetaine methacrylate-co-acrylic acid) to reduce fibrinogen adsorption, platelet adhesion, and plasma coagulation. Biomacromolecules 2011;12:4348–56.
[42] Chang Y, Shih YJ, Lai CJ, Kung HH, Jiang SY. Blood-inert surfaces via ion-pair anchoring of zwitterionic copolymer brushes in human whole blood. Adv Funct Mater 2013;23:1100–10.
[43] Cheng G, Zhang Z, Chen SF, Bryers JD, Jiang SY. Inhibition of bacterial adhesion and biofilm formation on zwitterionic surfaces. Biomaterials 2007;28:4192–9.
[44] Huang C-J, Brault ND, Li Y, Yu Q, Jiang S. Controlled hierarchical architecture in surface-initiated zwitterionic polymer brushes with structurally regulated functionalities. Adv Mater 2012;24:1834–7.
[45] Slaughter GE, Bieberich E, Wnek GE, Wynne KJ, Guiseppi-Elie A. Improving neuron-to-electrode surface attachment via alkanethiol self-assembly: an alternating current impedance study. Langmuir 2004;20:7189–200.
[46] Wisniewski N, Reichert M. Methods for reducing biosensor membrane biofouling. Colloids Surf, B 2000;18:197–219.
[47] Wang J. Electrochemical glucose biosensors. Chem Rev 2007;108:814–25.

Please cite this article in press as: Hu Y et al. The fabrication of superlow protein absorption zwitterionic coating by electrochemically mediated atom transfer radical polymerization and its application. Acta Biomater (2014), http://dx.doi.org/10.1016/j.actbio.2014.11.023